CrossMark

ORIGINAL PAPER

Studying linear and nonlinear vibrations of fractional viscoelastic Timoshenko micro-/nano-beams using the strain gradient theory

R. Ansari · M. Faraji Oskouie · H. Rouhi

Abstract In this paper, the vibrational behavior of micro- and nano-scale viscoelastic beams under different types of end conditions in the linear and nonlinear regimes is investigated based on the fractional calculus. To capture the effects of small scale, the modified strain gradient theory is utilized. Also, the beams are modeled based on the Timoshenko beam theory, von Kármán nonlinear relations and the fractional Kelvin–Voigt viscoelastic model. Derivation of governing equations is performed using Hamilton's principle. For the linear solution, the generalized differential quadrature and finite difference methods are employed. Moreover, in the nonlinear solution procedure, the Galerkin method is first used to convert the fractional integro-partial differential governing equations into fractional ordinary differential equations which are then arranged in an effective state-space form. The predictor–corrector technique is finally used to solve the set of nonlinear fractional time-dependent equations. Selected numerical results are given on the linear and nonlinear time responses of the fractional viscoelastic small-scale beams to study the effects of fractional-order, viscoelasticity coefficient and length scale parameter.

R. Ansari (✉) · M. Faraji Oskouie
Department of Mechanical Engineering,
University of Guilan, P.O. Box 3756, Rasht, Iran
e-mail: r_ansari@guilan.ac.ir

H. Rouhi
Department of Engineering Science, Faculty of Technology and Engineering, East of Guilan, University of Guilan, Rudsar-Vajargah 44891-63157, Iran

1 Introduction

In recent years, research into the mechanical behaviors of beam-type micro- and nano-structures has attracted considerable attention due to their several applications. A literature review on the studies performed on this issue shows that the majority of them are based on the continuum mechanics. The acceptability of continuum approaches can be attributed to their computational efficiency when they are compared with the atomistic approaches.

It has been proved that the mechanical behaviors of structures at small scales are size dependent [1–6], and continuum models used for the mechanical analyses of micro- and nano-structures must be size dependent in order to give accurate results. There are several size-dependent continuum theories by which the size effects can be incorporated into the continuum models. Among them, the surface stress [7,8], couple stress [9–11] and nonlocal [12] theories can be mentioned. Up to now, numerous applications of these theories to different problems of small-scale structures have been reported (e.g., [13–24]).

In the middle of 1960s, Mindlin [25,26] developed a size-dependent continuum theory called the strain gradient theory (SGT) in which the first and

 Springer

second derivatives of the strain tensor effective on the strain energy density were taken into account. In 2003, Lam et al. [27] made some modifications to this theory and proposed the modified strain gradient theory (MSGT). Based on MSGT, three length scale parameters corresponding to the dilatation gradient tensor, deviatoric gradient tensor and symmetric rotation gradient tensor are considered. One can find many papers in which MSGT has been used to capture the size effects on the mechanics of small-scale structures. For example, Ansari et al. [28] studied the size-dependent vibrations of curved micro-beams made of functionally graded materials (FGMs) based on MSGT. Akgöz and Civalek [29,30] investigated the buckling of micro-beams using MSGT. Abbasi and Karami Mohammadi [31] developed a strain gradient model to study the resonant frequency and sensitivity of atomic force microscopy micro-cantilevers. Instability of electrostatic nano-bridges and nano-cantilevers was analyzed by Tadi Beni et al. [32] within the framework of MSGT. Zeighampour and Tadi Beni [33] developed a strain gradient Euler–Bernoulli beam model in order to investigate the free vibrations of nano-beams made of FGMs with radius varying along the length. Mohammadimehr et al. [34] studied the free vibrations of double-bonded piezoelectric Timoshenko micro-beams based on MSGT and surface stress elasticity theory.

Recently, studying the mechanical behaviors of viscoelastic micro- and nano-structures based on the size-dependent continuum theories has attracted the attention of some researchers. Herein, some of them are cited. Lei et al. [35] studied the free vibration of damped viscoelastic Euler–Bernoulli beams based on the nonlocal theory and Kelvin–Voigt model. In another work, Lei et al. [36] developed a Timoshenko beam model to analyze the damped vibrations of nonlocal Kelvin–Voigt viscoelastic beams. The dynamic stability problem of viscoelastic nano-beams subjected to compressive axial loading was addressed by Pavlović et al. [37]. The Kelvin–Voigt model in conjunction with the nonlocal theory was applied for modeling the nano-beams in that work. Cajic et al. [38] investigated the free damped transverse vibrations of nano-beams based on the nonlocal theory and the fractional derivative viscoelasticity. In the context of nonlocal theory and fractional calculus, Ansari et al. [39,40] analyzed the linear and nonlinear vibrations of fractional viscoelastic nano-beams.

In the current work, the linear and nonlinear vibration characteristics of fractional viscoelastic micro-/nano-beams are studied within the framework of MSGT. The nonlinear fractional viscoelastic beam model is developed on the basis of the Timoshenko beam theory, von Kármán hypothesis and the Kelvin–Voigt model. Hamilton's principle is utilized to obtain the governing equations and associated boundary conditions which are then solved in the linear and nonlinear regimes. The GDQ and FD methods are employed for solving the linear problem. Moreover, solving the nonlinear problem is done using the Galerkin and predictor–corrector methods. In the numerical results, the effects of different parameters including fractional-order, length scale parameter and viscoelasticity coefficient on the time response of viscoelastic beams under different boundary conditions are analyzed.

2 Derivation of governing equations

Based on MSGT [27], the strain energy in a deformed isotropic linear elastic material occupying region Ω (with a volume element V) is given by

$$U = \frac{1}{2} \int_{\Omega} \left(\sigma_{ij} \varepsilon_{ij} + P_i \gamma_i + \tau_{ijk}^{(1)} \eta_{ijk}^{(1)} + m_{ij}^{S} \chi_{ij}^{S} \right) \mathrm{d}V \tag{1}$$

where the deformation measures, i.e., the strain tensor, ε_{ij}, the dilatation gradient tensor, γ_i, the deviatoric stretch gradient tensor, $\eta_{ijk}^{(1)}$, and the symmetric rotation gradient tensor, χ_{ij}^{S}, are defined as

$$\varepsilon_{ij} = \frac{1}{2} \left(u_{i,j} + u_{j,i} \right), \tag{2}$$

$$\gamma_i = \varepsilon_{mm,i}, \tag{3}$$

$$\eta_{ijk}^{(1)} = \frac{1}{3} \left(\varepsilon_{jk,i} + \varepsilon_{ki,j} + \varepsilon_{ij,k} \right)$$
$$- \frac{1}{15} \left[\delta_{ij} \left(\varepsilon_{mm,k} + 2\varepsilon_{mk,m} \right) \right.$$
$$+ \delta_{jk} \left(\varepsilon_{mm,i} + 2\varepsilon_{mi,m} \right)$$
$$\left. + \delta_{ki} \left(\varepsilon_{mm,j} + 2\varepsilon_{mj,m} \right) \right] \tag{4}$$

$$\chi_{ij}^{S} = \frac{1}{2} \left(e_{ipq} \varepsilon_{qj,p} + e_{jpq} \varepsilon_{qi,p} \right) \tag{5}$$

in which u_i denotes the displacement vector, ε_{mm} denotes the dilatation strain, and δ_{ij} and e_{ijk} denote the Kronecker delta and permutation tensor, respectively.

Throughout this paper, the repeated indices (subscripts) signify summation from 1 to 3.

The stress measures consist of the classical stress, σ_{ij}, and the higher-order stresses, P_i, $\tau_{ijk}^{(1)}$, and m_{ij}^S, which are the work-conjugate to the deformation measures, given by the following constitutive relations

$$\sigma_{ij} = 2\mu \left(\varepsilon_{ij} + \frac{v}{1-2v} \varepsilon_{mm} \delta_{ij} \right), \tag{6}$$

$$P_i = 2\mu l_0^2 \gamma_i, \tag{7}$$

$$\tau_{ijk}^{(1)} = 2\mu l_1^2 \eta_{ijk}^{(1)}, \tag{8}$$

$$m_{ij}^S = 2\mu l_2^2 \chi_{ij}, \tag{9}$$

In these relations, μ and v are shear modules and Poisson's ratio, respectively. Also, l_0, l_1 and l_2 are the additional and independent material length scale parameters associated with the dilatation gradients, and symmetric rotation gradients, respectively.

Consider a beam with length L, thickness h and width b. On the basis of the Timoshenko beam theory, the displacement field can be expressed as

$$u_1 = u(x,t) - z\psi(x,t), u_2 = 0, u_3 = W(x,t) \tag{10}$$

where u stands for the axial displacement of the centroid of sections and W is the lateral deflection of the beam. Using the von Kármán hypothesis, the strain components can be approximated as

$$\varepsilon_{11} = \frac{\partial u_1}{\partial x} + \frac{1}{2} \left(\frac{\partial W}{\partial x} \right)^2 = \frac{\partial u}{\partial x} + z\frac{\partial \psi}{\partial x} + \frac{1}{2} \left(\frac{\partial W}{\partial x} \right)^2,$$

$$\gamma_{12} = \frac{\partial W}{\partial x} + \psi \tag{11}$$

Using Hamilton's principle, the geometrically nonlinear governing equations of motion and boundary conditions of the beam with immovable supports are then derived as [41]

$$\overline{k_3} \left(\frac{\partial^2 W}{\partial x^2} + \frac{\partial \psi}{\partial x} \right) + \left(\overline{k_6} - \overline{k_7} \right) \frac{\partial^4 W}{\partial x^4}$$

$$+ \left(2\overline{k_6} + \overline{k_7} \right) \frac{\partial^3 \psi}{\partial x^3} \left[\frac{\overline{k_1}}{2L} \int_0^L \left(\frac{\partial W}{\partial x} \right)^2 \mathrm{d}x \right] \frac{\partial^2 W}{\partial x^2}$$

$$= \rho A \frac{\partial^2 W}{\partial t^2} - F \sin(\Omega t)$$

$$\overline{k_2} \frac{\partial^2 \psi}{\partial x^2} - \overline{k_3} \left(\frac{\partial W}{\partial x} + \psi \right) - \overline{k_4} \frac{\partial^4 \psi}{\partial x^4}$$

$$- \left(\overline{k_7} - 2\overline{k_6} \right) \frac{\partial^3 W}{\partial x^3} + \left(\overline{k_7} + 4\overline{k_6} \right) \frac{\partial^2 \psi}{\partial x^2} = \rho I \frac{\partial^2 \psi}{\partial t^2}$$

$$\left(\overline{k_2} \frac{\partial \psi}{\partial x} - \overline{k_4} \frac{\partial^3 \psi}{\partial x^3} + \left(\overline{k_7} - 2\overline{k_6} \right) \frac{\partial^2 W}{\partial x^2} \right.$$

$$\left. + \left(\overline{k_7} + 4\overline{k_6} \right) \frac{\partial \psi}{\partial x} \right) = 0 \ or \ \delta\psi = 0$$

$$\overline{k_3} \left(\frac{\partial W}{\partial x} + \psi \right) - \left(\overline{k_6} + \overline{k_7} \right) \frac{\partial^3 W}{\partial x^3}$$

$$+ \left(2\overline{k_6} - \overline{k_7} \right) \frac{\partial^2 \psi}{\partial x^2} = 0 \ or \ \delta W = 0$$

$$\overline{k_4} \frac{\partial^2 \psi}{\partial x^2} = 0 \ or \ \delta\left(\frac{\partial \psi}{\partial x} \right) = 0$$

$$\left(\overline{k_6} + \overline{k_7} \right) \frac{\partial^2 W}{\partial x^2} + \left(\overline{k_7} - 2\overline{k_6} \right) \frac{\partial \psi}{\partial x}$$

$$= 0 \ or \ \delta\left(\frac{\partial W}{\partial x} \right) = 0 \tag{12}$$

where $F \sin(\Omega t)$ is related to the forced vibration problem, and

$$\overline{k_1} = EA, \quad \overline{k_2} = EI + 2\mu A l_0^2, \quad \overline{k_3} = k_s \mu A,$$

$$\overline{k_4} = \mu I \left(2l_0^2 + \frac{4}{5}l_1^2 \right), \quad \overline{k_5} = \mu A \left(2l_0^2 + \frac{4}{5}l_1^2 \right),$$

$$\overline{k_6} = \frac{8}{15}\mu A l_1^2, \quad \overline{k_7} = \frac{1}{4}\mu A l_2^2 \tag{13}$$

Based on the fractional Kelvin–Voigt viscoelastic model, E and μ are replaced with $E\left(1 + \bar{g}\frac{\partial^\alpha}{\partial t^\alpha} \right)$ and $\mu\left(1 + \bar{g}\frac{\partial^\alpha}{\partial t^\alpha} \right)$, where $\bar{g}$ and α indicate the viscoelasticity coefficient and fractional derivative order, respectively. Furthermore, the fractional derivative is defined as [42]

$$D_t^\alpha(w) = I^{1-\alpha}(\dot{w}) = \frac{1}{\Gamma(1-\alpha)} \int_0^t \frac{w'(t-\tau)}{\tau^\alpha} \mathrm{d}\tau$$

$$+ \frac{w(0)}{\Gamma(1-\alpha)t^\alpha}, \quad 0 < \alpha < 1 \tag{14}$$

Accordingly, the governing equations of the fractional viscoelastic Timoshenko beam on the basis of the strain gradient theory and the Kelvin–Voigt linear viscoelastic model can be obtained as

$$\left(1 + \bar{g}\frac{\partial^\alpha}{\partial t^\alpha} \right) \left\{ \overline{k_3} \left(\frac{\partial^2 W}{\partial x^2} + \frac{\partial \psi}{\partial x} \right) \right.$$

$$+ \left(\overline{k_6} - \overline{k_7} \right) \frac{\partial^4 W}{\partial x^4} + \left(2\overline{k_6} + \overline{k_7} \right) \frac{\partial^3 \psi}{\partial x^3}$$

$$\left. + \left[\frac{\overline{k_1}}{2L} \int_0^L \left(\frac{\partial W}{\partial x} \right)^2 \mathrm{d}x \right] \frac{\partial^2 W}{\partial x^2} \right\}$$

$$= \rho A \frac{\partial^2 W}{\partial t^2} - F \sin(\Omega t) \tag{15a}$$

$$\left(1 + \bar{g} \frac{\partial^\alpha}{\partial t^\alpha}\right) \left[\overline{k_2} \frac{\partial^2 \psi}{\partial x^2} - \overline{k_3} \left(\frac{\partial W}{\partial x} + \psi \right) \right.$$

$$- \overline{k_4} \frac{\partial^4 \psi}{\partial x^4} - \left(\overline{k_7} - 2\overline{k_6} \right) \frac{\partial^3 W}{\partial x^3}$$

$$\left. + \left(\overline{k_7} + 4\overline{k_6} \right) \frac{\partial^2 \psi}{\partial x^2} \right] = \rho I \frac{\partial^2 \psi}{\partial t^2} \tag{15b}$$

Introducing the following dimensionless parameters

$$w = \frac{W}{L}, \zeta = \frac{x}{L}, O = L^2 \sqrt{\frac{\rho A}{EI}}, \{\ell_0, \ell_1, \ell_2\}$$

$$= \frac{\{l_0, l_1, l_2\}}{L}, \{\tau, g\} = \frac{\{t, \bar{g}\}}{O}, k_1 = \frac{AL^2}{I},$$

$$k_2 = \frac{\left(EI + 2\mu AL^2 \ell_0^2\right)}{EI}, k_3 = \frac{k_s \mu AL^2}{EI},$$

$$k_4 = \frac{\mu \left(2\ell_0^2 + \frac{4}{5}\ell_1^2\right)}{EI},$$

$$k_5 = \frac{\mu A \left(2\ell_0^2 + \frac{4}{5}\ell_1^2\right) L^2}{EI}, k_6 = \frac{8\mu AL^2 \ell_1^2}{15EI},$$

$$k_7 = \frac{\mu AL^2 \ell_2^2}{4EI},$$

$$f = \frac{FL^3}{EI}, \omega = \Omega \times O \tag{16}$$

Equation (15) can be rewritten in the following dimensionless form

$$\left(1 + g \frac{\partial^\alpha}{\partial \tau^\alpha}\right) \left[k_3 \left(\frac{\partial^2 w}{\partial \zeta^2} + \frac{\partial \psi}{\partial \zeta} \right) + (k_6 - k_7) \frac{\partial^4 w}{\partial \zeta^4} \right.$$

$$\left. + (2k_6 + k_7) \frac{\partial^3 \psi}{\partial \zeta^3} + \left[\frac{k_1}{2} \int_0^1 \left(\frac{\partial w}{\partial \zeta} \right)^2 d\zeta \right] \frac{\partial^2 w}{\partial \zeta^2} \right]$$

$$= \frac{\partial^2 W}{\partial \tau^2} + f \sin(\omega \tau) \tag{17a}$$

$$\left(1 + g \frac{\partial^\alpha}{\partial \tau^\alpha}\right) \left[k_2 \frac{\partial^2 \psi}{\partial x^2} - k_3 \left(\frac{\partial W}{\partial x} + \psi \right) \right.$$

$$- k_4 \frac{\partial^4 \psi}{\partial x^4} - (k_7 - 2k_6) \frac{\partial^3 W}{\partial x^3}$$

$$\left. + (k_7 + 4k_6) \frac{\partial^2 \psi}{\partial x^2} \right] = \frac{1}{k_1} \frac{\partial^2 \psi}{\partial \tau^2} \tag{17b}$$

3 Solution approaches

3.1 Linear analysis

First, the linear vibration problem of the fractional viscoelastic beam is solved. To this end, the governing equations are discretized by the GDQ and FD methods in space and time domains.

Based on the GDQ method [43], the rth-order derivative of function $f(x)$ including N grid points in the domain is approximated as

$$\left. \frac{\partial^r f(x)}{\partial x^r} \right|_{x=x_i} = \sum_{j=1}^N \mathcal{W}_{ij}^{(r)} f(x_j) \tag{18}$$

in which x_j signifies the coordinates of a discrete grid point in the variable domain, $f(x_j)$ represents the value of function at the grid point x_j, and $\mathcal{W}_{ij}^{(r)}$ denotes the corresponding weighting coefficients which is approximated through the following formula

$$\mathcal{W}_{ij}^{(r)} = \begin{cases} \mathbf{I}_x, & \text{where } \mathbf{I}_x \text{ is a } N \times N \text{ identity matrix}, r = 0 \\ \frac{\mathcal{P}(x_i)}{(x_i - x_j)\mathcal{P}(x_j)}, & \text{where } \mathcal{P}(x_i) = \prod_{j=1; j \neq i}^N (x_i - x_j), i \neq j \text{ and } i, j = 1, \dots, N \\ r \left[\mathcal{W}_{ij}^{(1)} \mathcal{W}_{ii}^{(r-1)} - \frac{\mathcal{W}_{ij}^{(r-1)}}{x_i - x_j} \right], i \neq j \text{ and } i, j = 1, \dots, N \text{ and } r = 2, 3, \dots N \\ -\sum_{j=1; j \neq i}^N \mathcal{W}_{ij}^{(r)}, i = j \text{ and } i, j = 1, \dots, N \text{ and } r = 1, 2, 3, \dots N - 1 \end{cases} \tag{19}$$

By inserting the function values $f(x_j)$ in a column vector as follows

$$\mathbf{F} = [f(x_1) \quad f(x_2) \quad \cdots \quad f(x_N)]^{\mathrm{T}} \tag{20}$$

Equation (18) is rewritten as

$$\frac{\mathrm{d}^r}{\mathrm{d}x^r} \mathbf{F} = \mathbf{D}_x^{(r)} \mathbf{F} \tag{21}$$

in which $\mathbf{D}_x^{(r)} = \left[\mathcal{W}_{ij}^{(r)} \right]$ is the operational matrix of differentiation, $i, j = 1, \dots, N$ and $r = 0, 1, 2, \dots, N-1$.

Now, the FD scheme is employed. The fractional-order derivative of a function at time t can be calculated according to the values of the function at times before t as [44]

$$\frac{1}{\Gamma(1-\alpha)}\int_0^{t_{k+1}}\frac{w'(t_{k+1}-\tau)}{\tau^\alpha}\mathrm{d}\tau$$
$$= \frac{\tau^\alpha}{\Gamma(2-\alpha)}\sum_{j=0}^k b_j^\alpha\left[w(t_{k+1-j})-w(t_{k-j})\right]$$
$$b_j^\alpha = (j+1)^{1-\alpha}-j^{1-\alpha}, \quad j=0,1,2,\ldots,n \quad (22)$$

In this equation, $0 < \alpha < 1$ is the order of fractional derivative, τ is time step, and $n+1$ is number of grid points.

In order to discretize the space domain, the grid points are generated via the shifted Chebyshev–Gauss–Lobatto equations as

$$\zeta_i = \frac{1}{2}\left(1-\cos\frac{i-1}{n-1}\pi\right), \quad i=1,2,3,\ldots,n \quad (23)$$

In addition, the grid points in the time domain are located with invariant distances given by

$$\tau_j = j\frac{T}{m+1}, \quad j=0,2,3,\ldots,m \quad (24)$$

Now, introducing matrices $\mathbf{W}$ and $\boldsymbol{\psi}$ as

$$\mathbf{W} = \begin{bmatrix} w_{10} & w_{12} & \cdots & w_{1n} \\ w_{20} & \ddots & \ddots & w_{2n} \\ \vdots & \ddots & \ddots & \vdots \\ w_{m0} & w_{m2} & \cdots & w_{mn} \end{bmatrix},$$

$$\boldsymbol{\psi} = \begin{bmatrix} \theta_{10} & \theta_{12} & \cdots & \theta_{1n} \\ \theta_{20} & \ddots & \ddots & \theta_{2n} \\ \vdots & \ddots & \ddots & \vdots \\ \theta_{m0} & \theta_{m2} & \cdots & \theta_{mn} \end{bmatrix},$$
$$i = 1\ldots m, \ j = 0\ldots n \quad (25)$$

in which $w_{ij} = w(x_i, t_j)$ and using the GDQ and FD methods, one can arrive at

$$\left[k_3\left(\mathbf{D}_\zeta^2\mathbf{W}\left(\mathbf{I}_t^\mathrm{T}+g\mathbf{D}_\tau^{\alpha\mathrm{T}}\right)+\mathbf{D}_\zeta^1\boldsymbol{\psi}\left(\mathbf{I}_t^\mathrm{T}+g\mathbf{D}_\tau^{\alpha\mathrm{T}}\right)\right)\right.$$
$$+(k_6-k_7)\mathbf{D}_\zeta^4\mathbf{W}\left(\mathbf{I}_t^\mathrm{T}+g\mathbf{D}_\tau^{\alpha\mathrm{T}}\right)$$
$$\left.+(2k_6+k_7)\mathbf{D}_\zeta^3\boldsymbol{\psi}\left(\mathbf{I}_t^\mathrm{T}+g\mathbf{D}_\tau^{\alpha\mathrm{T}}\right)\right]$$
$$+g\left(\frac{1}{\Gamma(1-\alpha)\tau^\alpha}\right)$$

$$\otimes\left(k_3\mathbf{D}_\zeta^1\boldsymbol{\psi_0}+k_3\mathbf{D}_\zeta^2\mathbf{W_0}+(k_6-k_7)\mathbf{D}_\zeta^4\mathbf{W_0}\right.$$
$$\left.+(2k_6+k_7)\mathbf{D}_\zeta^3\boldsymbol{\psi_0}\right)^T$$
$$= \mathbf{I}_\zeta\mathbf{W}\mathbf{D}_\tau^{2\mathrm{T}}+\sin(\omega\boldsymbol{\tau})\otimes\boldsymbol{f}(\zeta) \quad (26a)$$

$$\left[k_2\mathbf{D}_\zeta^2\boldsymbol{\psi}\left(\mathbf{I}_t^\mathrm{T}+g\mathbf{D}_\tau^{\alpha\mathrm{T}}\right)-k_3\left(\mathbf{D}_\zeta^1\mathbf{W}\left(\mathbf{I}_t^\mathrm{T}+g\mathbf{D}_\tau^{\alpha\mathrm{T}}\right)\right.\right.$$
$$\left.+\mathbf{I}_\zeta\boldsymbol{\psi}\left(\mathbf{I}_t^\mathrm{T}+g\mathbf{D}_\tau^{\alpha\mathrm{T}}\right)\right)-k_4\mathbf{D}_\zeta^4\boldsymbol{\psi}\left(\mathbf{I}_t^\mathrm{T}+g\mathbf{D}_\tau^{\alpha\mathrm{T}}\right)$$
$$-(k_7-2k_6)\mathbf{D}_\zeta^3\mathbf{W}\left(\mathbf{I}_t^\mathrm{T}+g\mathbf{D}_\tau^{\alpha\mathrm{T}}\right)$$
$$\left.+(k_7+4k_6)\mathbf{D}_\zeta^2\boldsymbol{\psi}\left(\mathbf{I}_t^\mathrm{T}+g\mathbf{D}_\tau^{\alpha\mathrm{T}}\right)\right]$$
$$+g\left(\frac{1}{\Gamma(1-\alpha)\tau^\alpha}\right)$$
$$\otimes\left(k_2\mathbf{D}_\zeta^2\boldsymbol{\psi_0}-k_3\mathbf{D}_\zeta^1\mathbf{W_0}-k_4\mathbf{D}_\zeta^4\boldsymbol{\psi_0}-k_3\mathbf{I}_\zeta\boldsymbol{\psi_0}\right.$$
$$\left.-(k_7-2k_6)\mathbf{D}_\zeta^3\mathbf{W_0}\right)^T$$
$$= \frac{1}{k_1}\mathbf{I}_\zeta\boldsymbol{\psi}\mathbf{D}_\tau^{2\mathrm{T}} \quad (26b)$$

$$\left(k_2\mathbf{D}_\zeta^1\boldsymbol{\psi}-k_4\mathbf{D}_\zeta^3\boldsymbol{\psi}+(k_7-2k_6)\mathbf{D}_\zeta^2\mathbf{W}+(k_7+4k_6)\mathbf{D}_\zeta^1\boldsymbol{\psi}\right)$$
$$\left(\mathbf{I}_t^\mathrm{T}+g\mathbf{D}_\tau^{\alpha\mathrm{T}}\right)=0 \quad \text{or} \quad \delta\psi=0 \quad (26c)$$

$$\left(k_3\left(\mathbf{D}_\zeta^1\mathbf{W}+\boldsymbol{\psi}\right)-(k_6+k_7)\mathbf{D}_\zeta^3\mathbf{W}+(2k_6-k_7)\mathbf{D}_\zeta^2\boldsymbol{\psi}\right)$$
$$\left(\mathbf{I}_t^\mathrm{T}+g\mathbf{D}_\tau^{\alpha\mathrm{T}}\right)=0 \quad \text{or} \quad \delta W=0 \quad (26d)$$

$$k_4\mathbf{D}_\zeta^2\boldsymbol{\psi}\left(\mathbf{I}_t^\mathrm{T}+g\mathbf{D}_\tau^{\alpha\mathrm{T}}\right)=0 \quad \text{or} \quad \delta\left(\mathbf{D}_\zeta^1\boldsymbol{\psi}\right)=0 \quad (26e)$$

$$\left((k_6+k_7)\mathbf{D}_\zeta^2\mathbf{W}+(k_7-2k_6)\mathbf{D}_\zeta^1\boldsymbol{\psi}\right)\left(\mathbf{I}_t^\mathrm{T}+g\mathbf{D}_\tau^{\alpha\mathrm{T}}\right)=0$$
$$\text{or} \quad \delta\left(\mathbf{D}_\zeta^1\mathbf{W}\right)=0 \quad (26f)$$

In these equations, $\boldsymbol{\psi_0}$ and $\mathbf{W_0}$ are the initial values of W and ψ; $\boldsymbol{\tau}$ is the vector of time; $\otimes$ shows the Kronecker product; $\mathbf{I}$ denotes the unit matrix; and $\mathbf{D}_t^\alpha$ is the fractional derivative operator of order α.

For solving Eqs. (26a) and (26b), both initial displacement and initial velocity must be known. Herein, the mode shape corresponding to the linear vibration of elastic beam is used as the initial displacement, and the initial velocity is considered to be zero. Then, by applying the discretized boundary conditions to the governing equations, an algebraic set of equations is achieved from which the unknown matrices $\mathbf{W}$ and $\boldsymbol{\psi}$ can be determined.

3.2 Nonlinear analysis

In this subsection, the nonlinear problem is solved. To accomplish this aim, the Galerkin method is utilized first so as to convert the fractional integro-partial differential governing equations into fractional ordinary

differential equations. In the next step, the obtained equations are arranged in an effective state-space form. Finally, the predictor–corrector method is used to solve the set of nonlinear fractional time-dependent equations and obtain the time response of fractional viscoelastic beam.

For the fractional viscoelastic beam under simply supported boundary conditions at two ends, the solution of Eq. (17) can be expressed as follows

$$w(\zeta,\tau) = \sum_{n=1}^{\infty} \varphi_n(\tau)\, p_n$$

$$\psi(\zeta,\tau) = \sum_{n=1}^{\infty} \theta_n(\tau)\, \Gamma_n \qquad (27)$$

in which $\varphi_n(\tau)$ indicates the time-dependent function; $p_n = \sin(n\pi\zeta)$ and $\Gamma_n = \cos(n\pi x)$ are the mode functions corresponding to the simply supported fractional viscoelastic beam. The function of exciting force is considered as $f = f_1 p_1(\zeta)$.

Substitution of Eq. (27) into (17) and applying the Galerkin method for the resulting equation give the following fractional ordinary differential equations

$$\left[k_3 \left(\left\{ \sum_{j=1}^{N} \int_0^1 p_i p_j'' \mathrm{d}\zeta \right\} \left(\varphi_j + \tau \varphi_j^{(\alpha)} \right) \right. \right.$$

$$+ \left. \left\{ \sum_{j=1}^{N} \int_0^1 p_i \Gamma_j' \mathrm{d}\zeta \right\} \left(\Theta_j + g\Theta_j^{(\alpha)} \right) \right)$$

$$+ (k_6 - k_7) \left\{ \sum_{j=1}^{N} \int_0^1 p_i p_j^{IV} \mathrm{d}\zeta \right\} \left(\varphi_j + \tau \varphi_j^{(\alpha)} \right)$$

$$+ (2k_6 + k_7) \left\{ \sum_{j=1}^{N} \int_0^1 p_i \Gamma_j''' \mathrm{d}\zeta \right\} \left(\Theta_j + g\Theta_j^{(\alpha)} \right)$$

$$+ \left\{ \frac{k_1}{2} \left\{ \sum_{j=1}^{N} \sum_{k=1}^{N} \sum_{l=1}^{N} \int_0^1 p_i p_j'' \mathrm{d}\zeta \int_0^1 p_k' p_l' \mathrm{d}\zeta \right\} \right.$$

$$\left. \left(\varphi_j \varphi_k \varphi_l + g \varphi_j \left(\varphi_k \varphi_l \right)^{(\alpha)} \right) \right\} \right]$$

$$= \left(\sum_{j=1}^{N} \int_0^1 p_i p_j \mathrm{d}\zeta \right) \ddot{\varphi}_j + \left(\sum_{j=1}^{N} \int_0^1 f_1 p_1 p_j \mathrm{d}\zeta \right)$$

$\sin(\omega\tau)$

$$\left[k_2 \left\{ \sum_{j=1}^{N} \int_0^1 \Gamma_i \Gamma_j'' \mathrm{d}\zeta \right\} \left(\Theta_j + g\Theta_j^{(\alpha)} \right) \right.$$

$$- k_3 \left(\left\{ \sum_{j=1}^{N} \int_0^1 \Gamma_i p_j' \mathrm{d}\zeta \right\} \left(\varphi_j + \tau \varphi_j^{(\alpha)} \right) \right.$$

$$+ \left. \left\{ \sum_{j=1}^{N} \int_0^1 \Gamma_i \Gamma_j \mathrm{d}\zeta \right\} \left(\Theta_j + g\Theta_j^{(\alpha)} \right) \right)$$

$$- k_4 \left\{ \sum_{j=1}^{N} \int_0^1 \Gamma_i \Gamma_j^{IV} \mathrm{d}\zeta \right\} \left(\Theta_j + g\Theta_j^{(\alpha)} \right)$$

$$- (k_7 - 2k_6) \left\{ \sum_{j=1}^{N} \int_0^1 \Gamma_i p_j''' \mathrm{d}\zeta \right\} \left(\varphi_j + g\varphi_j^{(\alpha)} \right)$$

$$+ \left. (k_7 + 4k_6) \left\{ \sum_{j=1}^{N} \int_0^1 \Gamma_i \Gamma_j'' \mathrm{d}\zeta \right\} \left(\Theta_j + g\Theta_j^{(\alpha)} \right) \right]$$

$$= \frac{1}{k_1} \left\{ \sum_{j=1}^{N} \int_0^1 \Gamma_i \Gamma_j \mathrm{d}\zeta \right\} \ddot{\Theta}_j \qquad (28)$$

Considering the following relations

$$X_{i1} = \varphi_i, \quad X_{i2} = \dot{\varphi}_i, \quad X_{i3} = \varphi_i^{(\alpha)},$$
$$X_{im} = (\varphi_i \varphi_{m-3})^{(\alpha)}, \quad X_{i5} = \theta_i,$$
$$X_{i6} = \dot{\theta}_i, \quad X_{i7} = \theta_i^{(\alpha)} \qquad (29)$$

Equation (28) can be expressed in the following state-space form

$$\frac{\partial X_{j1}}{\partial t} = X_{j2}$$

$$\frac{\partial X_{j2}}{\partial t} = \frac{\left[k_3 \left\{ \sum_{j=1}^{N} \int_0^1 p_i p_j'' \mathrm{d}\zeta \right\} (k_6 - k_7) \left\{ \sum_{j=1}^{N} \int_0^1 p_i p_j^{IV} \mathrm{d}\zeta \right\} \right] \left(X_{j1} + g \left(X_{j3} + \frac{X_{j1_0}}{\Gamma(1-\alpha)t^\alpha} \right) \right)}{\left(\sum_{j=1}^{N} \int_0^1 p_i p_j \mathrm{d}\zeta \right)}$$

$$+ \frac{\frac{k_1}{2} \left\{ \sum_{j=1}^{N} \sum_{k=1}^{N} \sum_{l=1}^{N} \int_0^1 p_i p_j'' \mathrm{d}\zeta \int_0^1 p_k' p_l' \mathrm{d}\zeta \right\} \left\{ X_{j1} X_{k1} X_{l1} + g X_{j1} \left(X_{km} + \frac{X_{k1_0} X_{m1_0}}{\Gamma(1-\alpha)t^\alpha} \right) \right\}}{\left(\sum_{j=1}^{N} \int_0^1 p_i p_j \mathrm{d}\zeta \right)}$$

$$+ \frac{\left[(2k_6 + k_7) + k_3 \left\{ \sum_{j=1}^{N} \int_0^1 \Gamma_i \Gamma_j' \mathrm{d}\zeta \right\} \right] \left\{ \sum_{j=1}^{N} \int_0^1 p_i \Gamma_j''' \mathrm{d}\zeta \right\} (X_{j5} + g X_{j7})}{\left(\sum_{j=1}^{N} \int_0^1 p_i p_j \mathrm{d}\zeta \right)}$$

$$+ \frac{\left(\sum_{j=1}^{N} \int_0^1 f_1 p_1 p_j \mathrm{d}\zeta \right) \sin(X_8)}{\left(\sum_{j=1}^{N} \int_0^1 p_i p_j \mathrm{d}\zeta \right)}$$

$$\frac{\partial^{1-\alpha} X_{i3}}{\partial t^{1-\alpha}} = X_{i2}$$

$$\frac{\partial^{1-\alpha} X_{im}}{\partial t^{1-\alpha}} = X_{i1} X_{(m-3)2} + X_{(m-3)1} X_{i2}$$

$$\frac{\partial X_{i5}}{\partial t} = X_{i6}$$

$$\frac{\partial X_{i6}}{\partial t} = \frac{\left[-k_4 \left\{ \sum_{j=1}^{N} \int_0^1 \Gamma_i \Gamma_j^{IV} \mathrm{d}\zeta \right\} + (k_7 + 4k_6 + k_2) \left\{ \sum_{j=1}^{N} \int_0^1 \Gamma_i \Gamma_j'' \mathrm{d}\zeta \right\} - k_3 \left\{ \sum_{j=1}^{N} \int_0^1 \Gamma_i \Gamma_j \mathrm{d}\zeta \right\} \right] (X_{j5} + g X_{j7})}{\frac{1}{k_1} \left\{ \sum_{j=1}^{N} \int_0^1 \Gamma_i \Gamma_j \mathrm{d}\zeta \right\}}$$

$$+ \frac{\left[-k_3 \left\{ \sum_{j=1}^{N} \int_0^1 \Gamma_i p_j' \mathrm{d}\zeta \right\} - (k_7 - 2k_6) \left\{ \sum_{j=1}^{N} \int_0^1 \Gamma_i p_j''' \mathrm{d}\zeta \right\} \right] \left\{ X_{j1} + g \left(X_{j3} + \frac{X_{j1_0}}{\Gamma(1-\alpha)t^\alpha} \right) \right\}}{\frac{1}{k_1} \left\{ \sum_{j=1}^{N} \int_0^1 \Gamma_i \Gamma_j \mathrm{d}\zeta \right\}}$$

$$\frac{\partial^{1-\alpha} X_{i7}}{\partial t^{1-\alpha}} = X_{i6}$$

$$\frac{\partial X_8}{\partial t} = \omega$$

$$(30)$$

The predictor–corrector method [45] is used to solve this set of nonlinear fractional ordinary equations in the time domain. Consider the fractional differential equation and corresponding initial conditions as

$$\begin{cases} D^\alpha x(t) = f(t, x(t)), \ 0 \le t < T \\ x^{(k)}(0) = x_0^{(k)}, \qquad k = 0, 1, 2, \dots, n-1 \end{cases}$$

$$(31)$$

where $n = \lceil \alpha \rceil$ shows the first integer which is not less than α and $\alpha > 0$, but not necessarily $\alpha \in N$. Moreover, $x^{(k)}$ is the ordinary kth derivative of $x(t)$.

Equation (31) can be rewritten as an equivalent Volterra integral equation and is defined by the following equation

$$x(t) = \sum_{k=0}^{n-1} \frac{x_0^{(k)} t^k}{k!} + \frac{1}{\Gamma(\alpha)} \int_0^t (t-\tau)^{\alpha-1} f(\tau, x(t)) \mathrm{d}\tau$$

$$(32)$$

The integral form of fractional governing equation can be discretized in the time domain. To this end, the time domain grid points are written as

$$t_j = j \times t_s; \quad t_s = \frac{T}{N}, \quad j = 0, 1, 2, \dots, N \in Z^+$$

$$(33)$$

where N denotes the number of total grid points. For the discretized form of Eq. (32), one has

$$x_h(t_{n+1}) = \sum_{k=0}^{\lceil \alpha \rceil - 1} \frac{x_0^{(k)} t^k}{k!}$$
$$+ \frac{t_s^\alpha}{\Gamma(\alpha+2)} f\left(t_{n+1}, x_h^p(t_{n+1})\right)$$
$$+ \frac{t_s^\alpha}{\Gamma(\alpha+2)} \sum_{j=0}^{n} a_{j,n+1} f\left(t_j, x_h(t_j)\right)$$
$$a_{j,n+1} = \begin{cases} n^{\alpha+1} - (n-\alpha)(n+1)^\alpha, & j = 0 \\ (n-j+2)^{\alpha+1} + (n-j)^{\alpha+1} - 2(n-j+1)^{\alpha+1}, & 1 \le j \le n \\ 1, & j = n+1 \end{cases}$$
$$x_h^p(t_{n+1}) = \sum_{k=0}^{\lceil \alpha \rceil - 1} \frac{x_0^{(k)} t^k}{k!}$$
$$+ \frac{1}{\Gamma(\alpha)} \sum_{j=0}^{n} b_{j,n+1} f\left(t_j, x_h(t_j)\right)$$
$$b_{j,n+1} = \frac{t_s^\alpha}{\alpha}\left((n-j+1)^\alpha - (n-j)^\alpha\right), \quad 1 \le j \le n \tag{34}$$

The aforementioned procedure is the well-known Adams–Bashforth–Moulton predictor–corrector scheme [46–48].

4 Results and discussion

In this section, selected numerical results are presented on the linear and nonlinear time responses of the fractional viscoelastic small-scale beams. C-C, C-SS and SS-SS end conditions are considered (simply supported and clamped ends are abbreviated to SS and C, respectively). It is assumed that $E = 427\,\text{GPa}$, $\nu = 0.17$ and $\rho = 3100\,\text{kg/m}^3$ [41].

Lam et al. [27] conducted experimental tests to evaluate the length scale parameter for an isotropic homogeneous micro-beam. They assumed that all the material length scale parameters are the same, i.e., $l_0 = l_1 = l_2 = l$, and obtained $l = 17.6\,\mu\text{m}$. However, to the authors' knowledge, there are no available experimental data for the length scale parameters of viscoelastic micro-beams in the open literature. Hence, in order to quantitatively investigate the size effect on the behavior of viscoelastic small-scale beams, the values of length scale parameters are approximately assumed to be equal to $l_0 = l_1 = l_2 = l = 15\,\mu\text{m}$ in the following examples. It should be noted that by choosing these parameters equal to zero, the governing equations based on the classical elasticity theory will be achieved. Also, by letting $l_0 = l_1 = 0$ and $l_2 = l$, the governing

equations based on modified couple stress theory are obtained.

In Fig. 1, the nonlinear time responses of free vibration of SS-SS beam based on different numbers of terms used in the Galerkin method [see Eq. (27)] are shown. It is observed that there is no considerable difference between the results corresponding to different numbers of terms employed in the Galerkin procedure. Therefore, one term will be used to generate the results provided.

In addition, in Fig. 2, the convergence of results is checked in which the linear time response of free vibration of SS-SS beam is shown for different numbers of grid points. This figure indicates quite clearly the converging trend of the present numerical approach. Besides, one can find that 13 grid points are enough to obtain converged results.

The influence of time step size is shown in Fig. 3. The calculations reveal that by choosing the time step larger than 0.001, the solution becomes unstable. But, for time steps smaller than 0.001, stable solutions are obtained. As shown in Fig. 3, there is no significant difference between the results by selecting different time steps smaller than 0.001, so the time step is taken to be 0.001.

In Fig. 4, the time responses of the SS-SS beam obtained by the FD and predictor–corrector methods are shown for different fractional orders. It is observed that there is a good agreement between the results of two solution methods.

In Fig. 5, the linear time response of the SS-SS beam is compared with its nonlinear time responses for various initial displacement values. It is seen that as the initial displacement decreases, the nonlinear frequency tends to decrease and the effect of geometrical nonlinearity diminishes so that the linear and nonlinear curves tend to converge.

Figures 6 and 7 show the influence of fractional order on the time response of beams. Three values for the fractional order including 0.3, 0.6 and 0.9 are considered. One can find that the frequency of the system decreases with increasing α. It is also seen that the decrease in maximum amplitude is intensified as this parameter gets larger. By elapsing time and the increase in damping due to increasing fractional order, the difference between the curves increases.

The effect of dimensionless viscoelasticity coefficient (g) on the vibrational behavior of beams is shown in Figs. 8 and 9. It is observed that increasing the viscoelasticity coefficient damps the vibrational
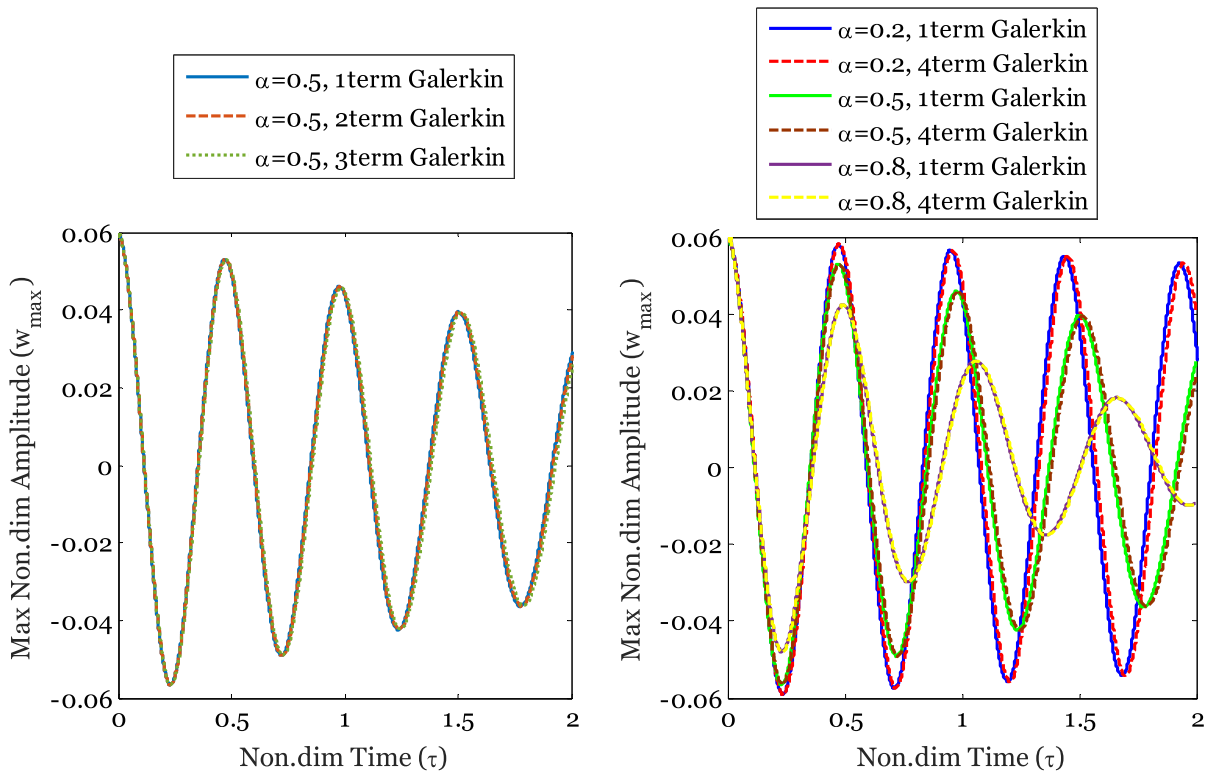
Fig. 1 Nonlinear time response of free vibration of the SS-SS fractional viscoelastic beam obtained by different numbers of terms used in the Galerkin method $\left(g = 0.03, \frac{h}{l} = 1 \right)$

Fig. 2 Linear time response of free vibration of the SS-SS fractional viscoelastic beam obtained by different numbers of grid points $\left(\alpha = 0.5, g = 0.03, \frac{h}{l} = 1 \right)$
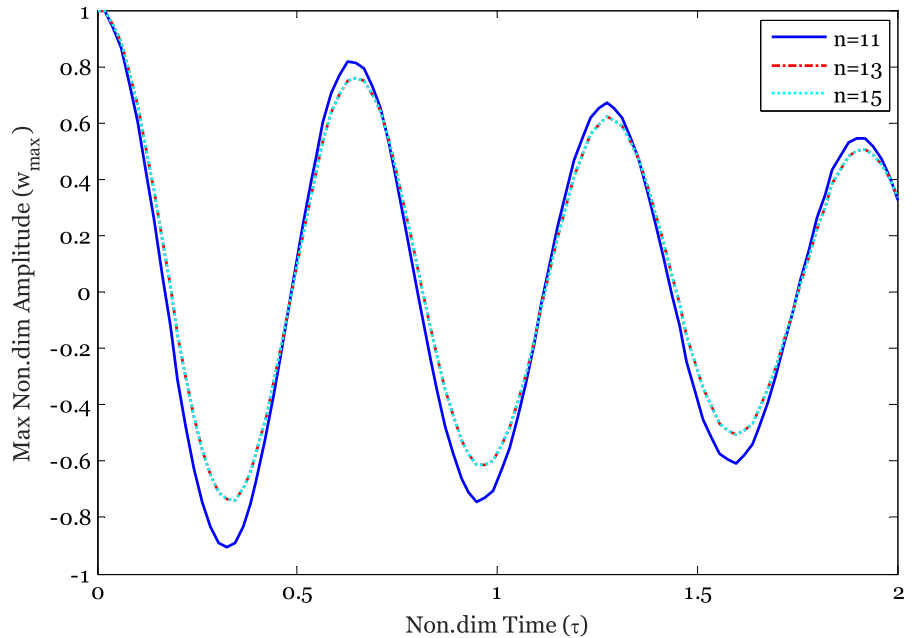
Fig. 3 Nonlinear time
response of free vibration of
the SS-SS fractional
viscoelastic beam obtained
based on different time steps
$\left(\alpha = 0.5, g = 0.03, \frac{h}{l} = 1\right)$
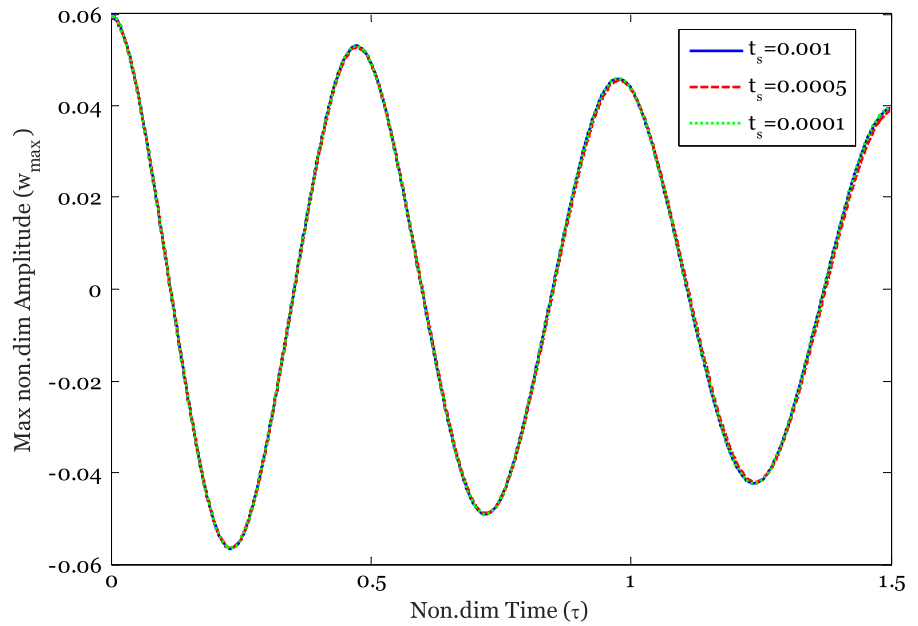
Fig. 4 Time response of
free vibration of the SS-SS
fractional viscoelastic beam
obtained by the FD and
predictor–corrector methods
for different fractional
orders $\left(g = 0.03, \frac{h}{l} = 1,\right.$
$\left.\frac{L}{h} = 10, b = 2h\right)$
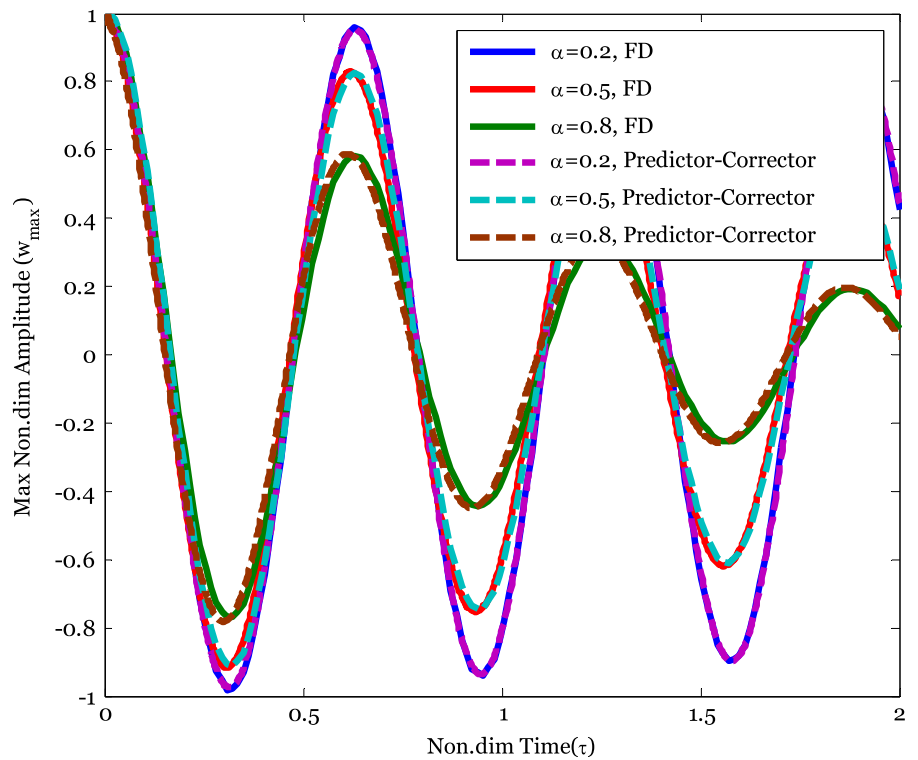
behavior of the system. This damping is intensified
by elapsing time. As it is expected, by elapsing time
and the decrease in maximum amplitude, the frequency
decreases more.

Figures 10 and 11 show the time response of beams
for different dimensionless length scale parameters
defined as h/l. In fact, the influence of small scale
on the size-dependent behavior of the system can be

Fig. 5 Comparison between the linear and nonlinear time responses of free vibration of SS-SS fractional viscoelastic beam with different initial displacements $\left(\frac{h}{l} = 1, \frac{L}{h} = 10, \alpha = 0.5, b = 2h\right)$
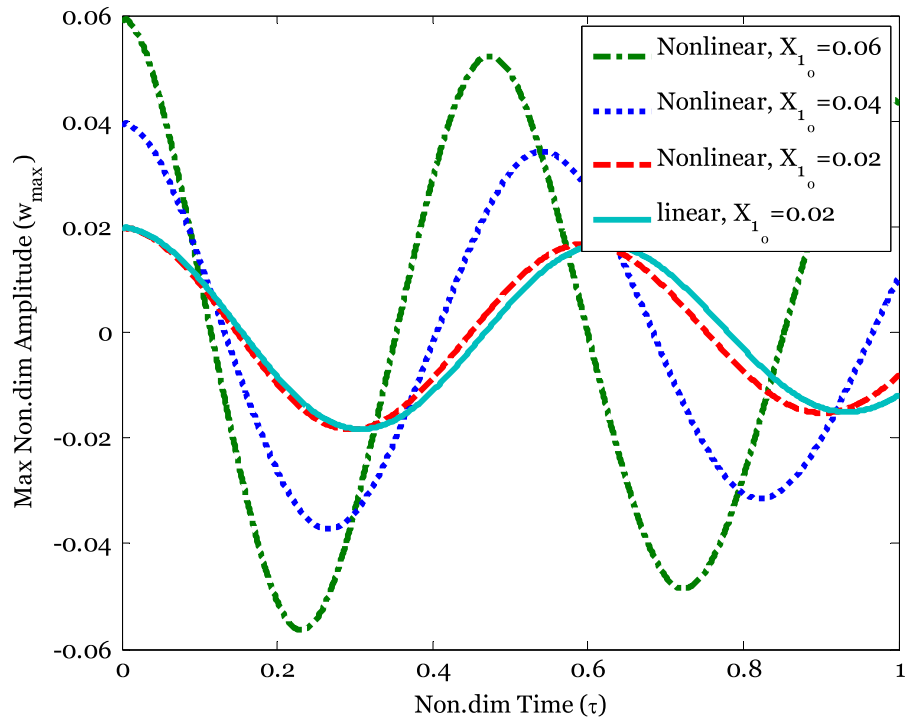
Fig. 6 Effect of fractional order on the nonlinear time response of free vibration of the fractional viscoelastic beam with SS-SS boundary conditions $\left(\frac{h}{l} = 1, \frac{L}{h} = 10, g = 0.03\right)$
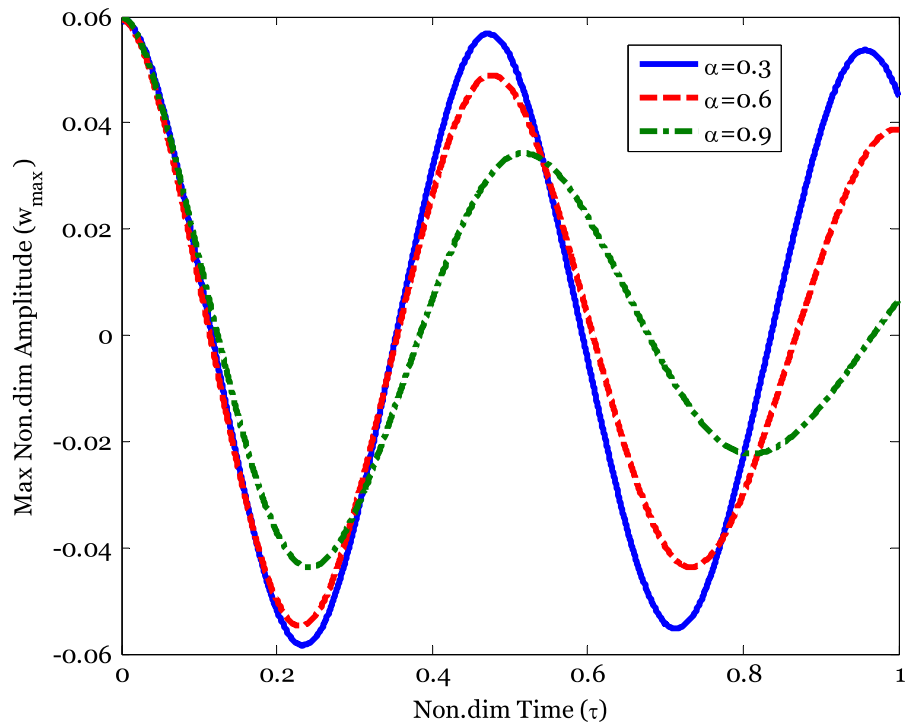

studied in these figures. The results indicate that with decreasing dimensionless length scale parameter, the frequency of the system increases. Also, the maximum amplitude in each period decreases to a lesser extent as h/l decreases.

Fig. 7 Effect of fractional order on the linear time response of free vibration of the fractional viscoelastic beams with **a** C-C, **b** C-SS, **c** SS-SS boundary conditions $\left(\frac{h}{l} = 1, \frac{L}{h} = 10, g = 0.03\right)$
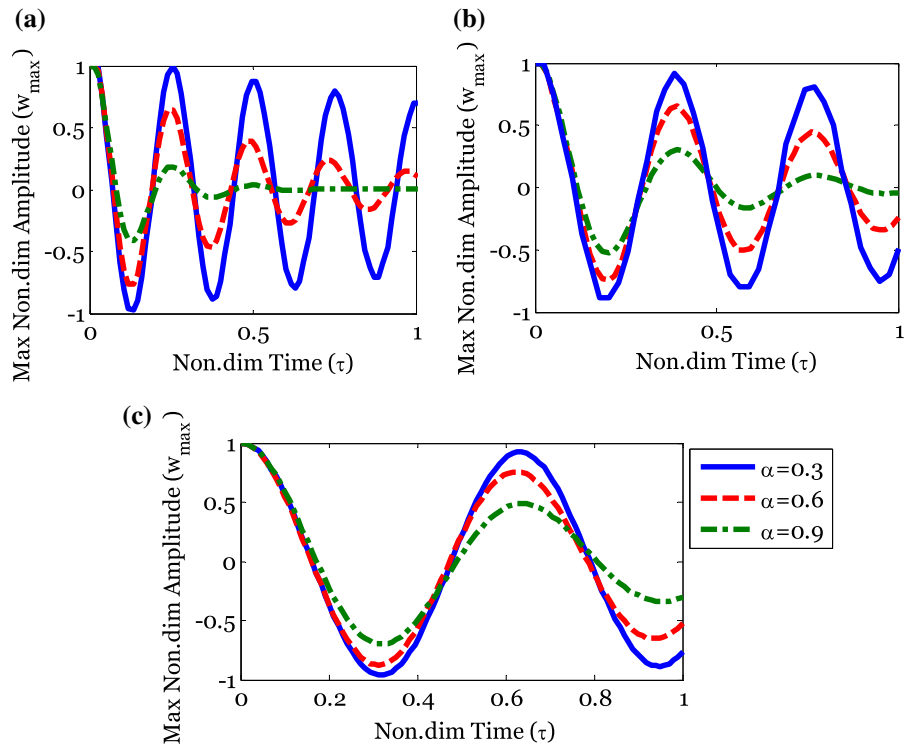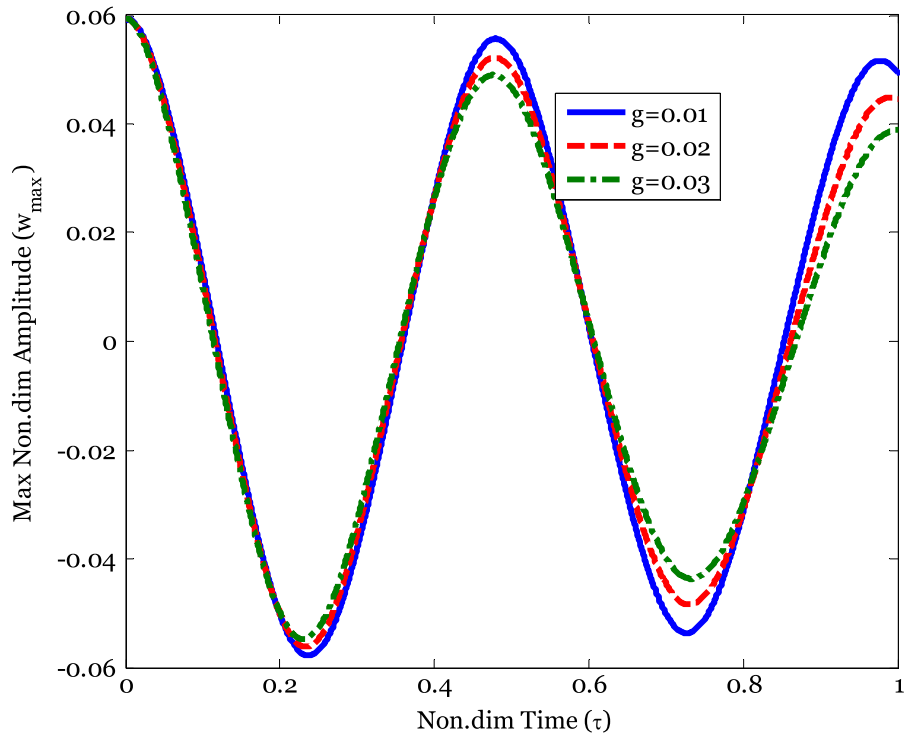

Fig. 8 Effect of non-dimensional viscoelasticity coefficient on the nonlinear time response of free vibration of the fractional viscoelastic beam with SS-SS boundary conditions $\left(\alpha = 0.6, \frac{h}{l} = 1, \frac{L}{h} = 10, b = 2h\right)$

Fig. 9 Effect of non-dimensional viscoelasticity coefficient on the linear time response of free vibration of the fractional viscoelastic beams with **a** C-C, **b** C-SS, **c** SS-SS boundary conditions $\left(\alpha = 0.5, \frac{h}{l} = 1, \frac{L}{h} = 10, \ b = 2h\right)$
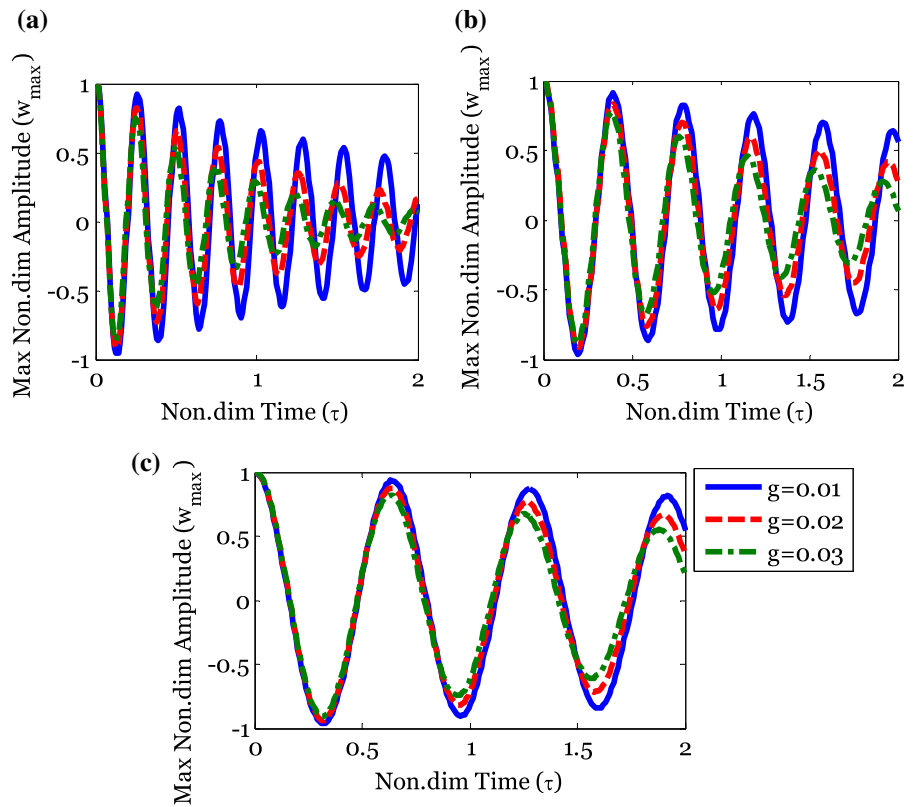

Fig. 10 Effect of dimensionless length scale parameter on the nonlinear time response of free vibration of the fractional viscoelastic beam with SS-SS boundary conditions $\left(\alpha = 0.5, \frac{L}{h} = 10, \ g = 0.03\right)$
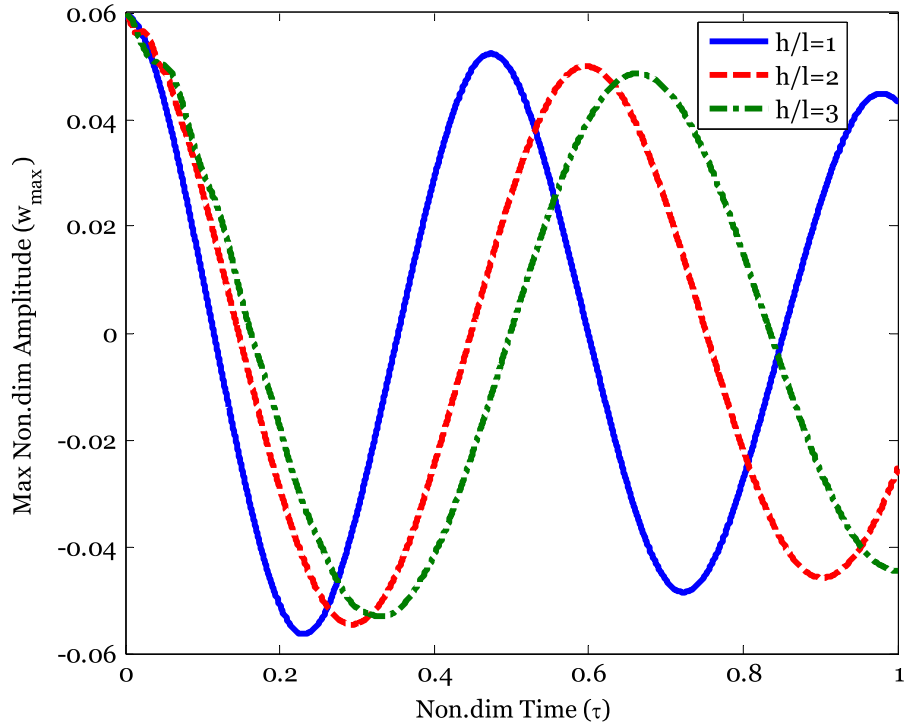
Fig. 11 Effect of dimensionless length scale parameter on the linear time response of free vibration of the fractional viscoelastic beams with **a** C-C, **b** C-SS, **c** SS-SS boundary conditions ($\alpha = 0.5$, $g = 0.03$, $\frac{L}{h} = 10$, $b = 2h$)
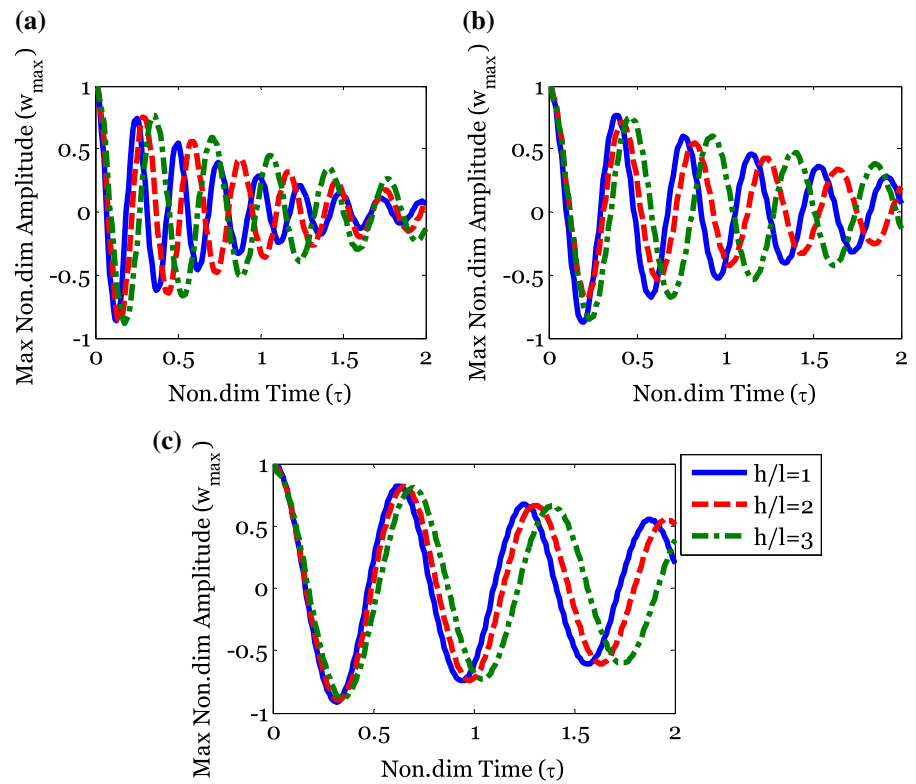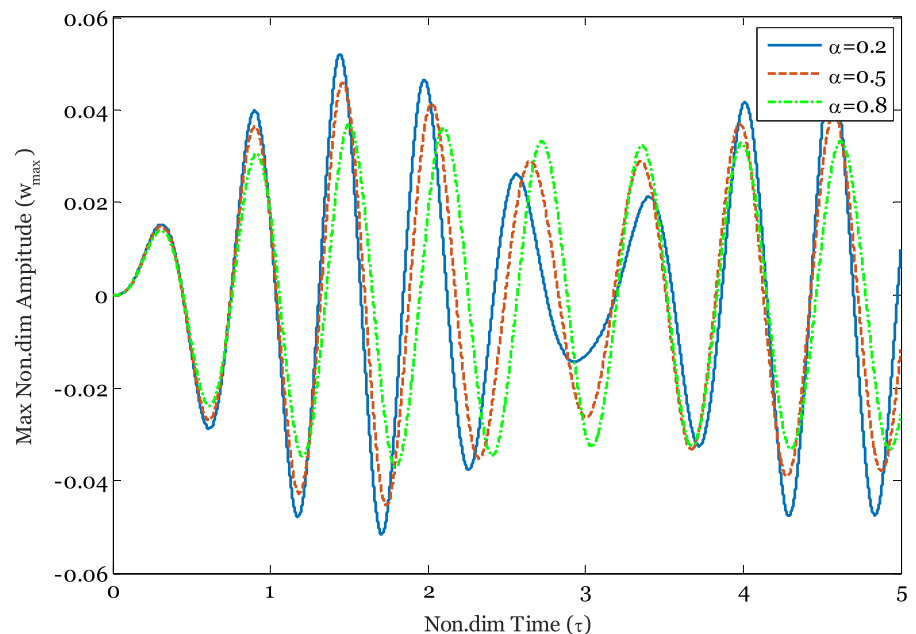

Fig. 12 Effect of fractional order on the nonlinear time response of forced vibration of fractional viscoelastic beams with SS-SS boundary conditions ($\omega = 10$, $g = 0.03$, $f_1 = 1$, $\frac{h}{l} = 1$, $\frac{L}{h} = 10$)

The nonlinear time responses of forced vibration of fractional viscoelastic beams are also illustrated in Figs. 12 and 13. From Fig. 12, one can find that changes in the maximum amplitude of vibration increase with decreasing fractional order. Also, increasing this para-meter leads to the increase in period of vibration. The influence of viscoelasticity coefficient on the nonlinear time response of forced vibration is also shown in Fig. 13.

Fig. 13 Effect of viscoelasticity parameter on the nonlinear time response of forced vibration of fractional viscoelastic beams with SS-SS boundary conditions $\left(\omega = 10, \alpha = 0.5, f_1 = 1, \frac{h}{l} = 1, \frac{L}{h} = 10\right)$
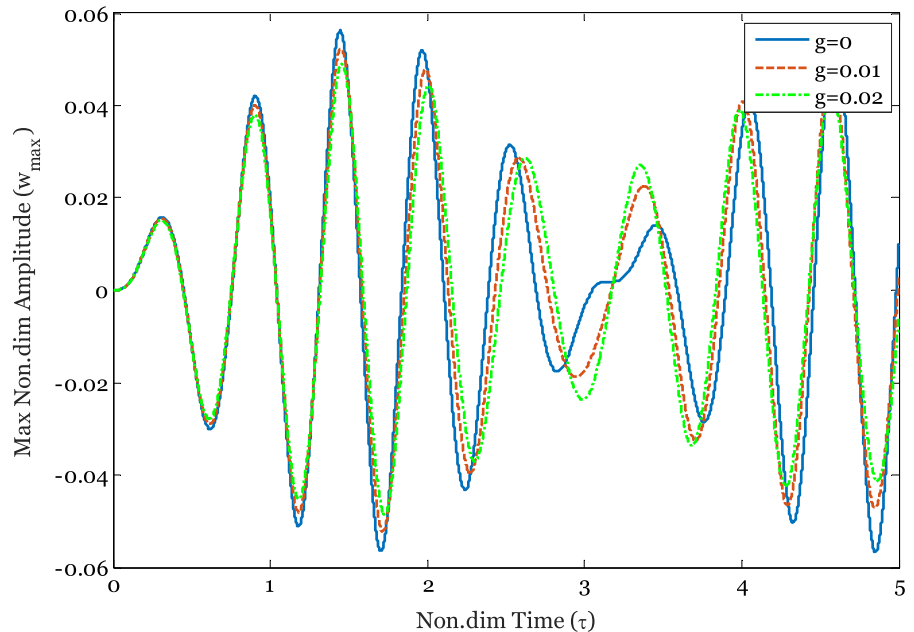
5 Conclusion

In the context of strain gradient theory, the size-dependent free and forced vibrations of fractional viscoelastic small-scale beams were studied in this article. The formulation was based on the Timoshenko beam theory, von Kármán geometrical nonlinear relations and the fractional Kelvin–Voigt viscoelastic model. After deriving the size-dependent governing equations, two solution approaches were employed to solve the linear and nonlinear vibration problems. In the linear solution, the GDQ and FD methods were employed in order to discretize the governing equations and boundary conditions. In the nonlinear solution approach, the Galerkin method was used to convert the fractional integro-partial differential governing equations into fractional ordinary differential equations that were then written in an effective state-space form. The predictor–corrector technique was also used to solve the set of nonlinear fractional time-dependent equations. The influences of fractional-order, viscoelasticity coefficient and length scale parameters on the linear and nonlinear time responses of the fractional viscoelastic small-scale beams were examined. It was observed that the frequency of the viscoelastic small-scale beams decreases as the fractional order increases. In addition, the damping of vibrations of system with increasing the viscoelasticity coefficient was shown. It was also revealed that the frequency of the system increases with decreasing thickness-to-length scale parameter ratio.

References

1. Nix, W.D., Gao, H.: Indentation size effects in crystalline materials: a law for strain gradient plasticity. J. Mech. Phys. Solids **46**, 411–425 (1998)
2. Fleck, N.A., Muller, G.M., Ashby, M.F., Hutchinson, J.W.: Strain gradient plasticity: theory and experiment. Acta Metall. Mater. **42**, 475–487 (1994)
3. Fleck, N.A., Hutchinson, J.W.: A reformulation of strain gradient plasticity. J. Mech. Phys. Solids **49**, 2245–2271 (2001)
4. McFarland, A.W., Colton, J.S.: Role of material microstructure in plate stiffness with relevance to microcantilever sensors. J. Micromech. Microeng. **15**, 1060–1067 (2005)
5. Mirnezhad, M., Ansari, R., Rouhi, H.: Effects of hydrogen adsorption on mechanical properties of chiral single-walled zinc oxide nanotubes. J. Appl. Phys. **111**, 0143082012 (2012)
6. Ansari, R., Mirnezhad, M., Rouhi, H.: Mechanical properties of chiral silicon carbide nanotubes under hydrogen adsorption: a molecular mechanics approach. NANO **9**, 1450043 (2014)
7. Gurtin, M.E., Murdoch, A.I.: A continuum theory of elastic material surfaces. Arch. Ration. Mech. Anal. **57**, 291–323 (1975)
8. Gurtin, M.E., Murdoch, A.I.: Surface stress in solids. Int. J. Solids Struct. **14**, 431–440 (1978)

9. Mindlin, R.D., Tiersten, H.F.: Effects of couple-stresses in linear elasticity. Arch. Ration. Mech. Anal. **11**, 415–448 (1962)

10. Koiter, W.T.: Couple stresses in the theory of elasticity. Proc. Koninklijke Nederl. Akad. van Wetensch (B) **67**, 17–44 (1964)

11. Yang, F., Chong, A.C.M., Lam, D.C.C., Tong, P.: Couple stress based strain gradient theory for elasticity. Int. J. Solids Struct. **39**, 2731–2743 (2002)

12. Eringen, A.C.: Nonlocal Continuum Field Theories. Springer, New York (2002)

13. Rouhi, H., Ansari, R.: Nonlocal analytical Flugge shell model for axial buckling of double-walled carbon nanotubes with different end conditions. NANO **7**, 1250018 (2012)

14. Ansari, R., Rouhi, H.: Explicit analytical expressions for the critical buckling stresses in a monolayer graphene sheet based on nonlocal elasticity. Solid State Commun. **152**, 56–59 (2012)

15. Akgöz, B., Civalek, Ö.: Free vibration analysis of axially functionally graded tapered Bernoulli–Euler microbeams based on the modified couple stress theory. Compos. Struct. **98**, 314–322 (2013)

16. Liang, Y., Han, Q.: Prediction of the nonlocal scaling parameter for graphene sheet. Eur. J. Mech. A/Solids **45**, 153–160 (2014)

17. Ansari, R., Faghih Shojaei, M., Rouhi, H.: Small-scale Timoshenko beam element. Eur. J. Mech. A/Solids **53**, 19–33 (2015)

18. Lei, J., He, Y., Zhang, B., Liu, D., Shen, L., Guo, S.: A size-dependent FG micro-plate model incorporating higher-order shear and normal deformation effects based on a modified couple stress theory. Int. J. Mech. Sci. **104**, 8–23 (2015)

19. Zeighampour, H., Tadi Beni, Y., Mehralian, F.: A shear deformable conical shell formulation in the framework of couple stress theory. Acta Mech. **226**, 2607–2629 (2015)

20. Ansari, R., Ashrafi, M.A., Arjangpay, A.: An exact solution for vibrations of postbuckled microscale beams based on the modified couple stress theory. Appl. Math. Model. **39**, 3050–3062 (2015)

21. Zeighampour, H., Tadi Beni, Y.: A shear deformable cylindrical shell model based on couple stress theory. Arch. Appl. Mech. **85**, 539–553 (2015)

22. Rouhi, H., Ansari, R., Darvizeh, M.: Size-dependent free vibration analysis of nanoshells based on the surface stress elasticity. Appl. Math. Model. **40**, 3128–3140 (2016)

23. Rouhi, H., Ansari, R., Darvizeh, M.: Analytical treatment of the nonlinear free vibration of cylindrical nanoshells based on a first-order shear deformable continuum model including surface influences. Acta Mech. **227**, 1767–1781 (2016)

24. Mercan, K., Civalek, Ö.: DSC method for buckling analysis of boron nitride nanotube (BNNT) surrounded by an elastic matrix. Compos. Struct. **143**, 300–309 (2016)

25. Mindlin, R.D.: Micro-structure in linear elasticity. Arch. Ration. Mech. Anal. **6**, 51–78 (1964)

26. Mindlin, R.D.: Second gradient of strain and surface tension in linear elasticity. Int. J. Solids Struct. **1**, 417–438 (1965)

27. Lam, D.C.C., Yang, F., Chong, A.C.M., Wang, J., Tong, P.: Experiments and theory in strain gradient elasticity. J. Mech. Phys. Solids **51**, 1477–1508 (2003)

28. Ansari, R., Gholami, R., Sahmani, S.: Size-dependent vibration of functionally graded curved microbeams based on the modified strain gradient elasticity theory. Arch. Appl. Mech. **83**, 1439–1449 (2013)

29. Akgöz, B., Civalek, Ö.: Buckling analysis of functionally graded microbeams based on the strain gradient theory. Acta Mech. **224**, 2185–2201 (2013)

30. Akgöz, B., Civalek, Ö.: A new trigonometric beam model for buckling of strain gradient microbeams. Int. J. Mech. Sci. **81**, 88–94 (2014)

31. Abbasi, M., Karami Mohammadi, A.: Study of the sensitivity and resonant frequency of the flexural modes of an atomic force microscopy microcantilever modeled by strain gradient elasticity theory. Proc. Inst. Mech. Eng. Part C J. Mech. Eng. Sci. **228**, 1299–1310 (2014)

32. Tadi Beni, Y., Karimipour, I., Abadyan, M.: Modeling the instability of electrostatic nano-bridges and nano-cantilevers using modified strain gradient theory. Appl. Math. Model. **39**, 2633–2648 (2015)

33. Zeighampour, H., Tadi Beni, Y.: Free vibration analysis of axially functionally graded nanobeam with radius varies along the length based on strain gradient theory. Appl. Math. Model. **39**, 5354–5369 (2015)

34. Mohammadimehr, M., Mohammadi Hooyeh, H., Afshari, H., Salarkia, M.R.: Free vibration analysis of double-bonded isotropic piezoelectric Timoshenko micro-beam based on strain gradient and surface stress elasticity theories under initial stress using DQM. Adv. Mater. Struct. Mech. (2016). doi:10.1080/15376494.2016.1142022

35. Lei, Y., Murmu, T., Adhikari, S., Friswell, M.I.: Dynamic characteristics of damped viscoelastic nonlocal Euler–Bernoulli beams. Eur. J. Mech. A/Solids **42**, 125–136 (2013)

36. Lei, Y., Adhikari, S., Friswell, M.I.: Vibration of nonlocal Kelvin–Voigt viscoelastic damped Timoshenko beams. Int. J. Eng. Sci. **66**, 1–13 (2013)

37. Pavlović, I., Pavlović, R., Ćirić, I., Karličić, D.: Dynamic stability of nonlocal Voigt–Kelvin viscoelastic Rayleigh beams. Appl. Math. Model. **39**, 6941–6950 (2015)

38. Cajic, M., Karlicic, D., Lazarevic, M.: Nonlocal vibration of a fractional order viscoelastic nanobeam with attached nanoparticle. Theor. Appl. Mech. **42**, 167–190 (2015)

39. Ansari, R., Faraji Oskouie, M., Sadeghi, F., Bazdid-Vahdati, M.: Free vibration of fractional viscoelastic Timoshenko nanobeams using the nonlocal elasticity theory. Phys. E **74**, 318–327 (2015)

40. Ansari, R., Faraji Oskouie, M., Gholami, R.: Size-dependent geometrically nonlinear free vibration analysis of fractional viscoelastic nanobeams based on the nonlocal elasticity theory. Phys. E **75**, 266–271 (2016)

41. Ansari, R., Gholami, R., Darabi, M.A.: A nonlinear Timoshenko beam formulation based on strain gradient theory. J. Mech. Mater. Struct. **7**, 195–211 (2012)

42. Grzesikiewicz, W., Wakulicz, A., Zbiciak, A.: Non-linear problems of fractional calculus in modeling of mechanical systems. Int. J. Mech. Sci. **70**, 90–98 (2013)

43. Shu, C.: Differential Quadrature and Its Application in Engineering. Springer, London (2000)

44. Liu, F., Meerschaert, M.M., McGough, R.J., Zhuang, P., Liu, Q.: Numerical methods for solving the multi-term time-fractional wave-diffusion equation. Fract. Calc. Appl. Anal. **16**, 9–25 (2013)

45. Sun, K., Wang, X., Sprott, J.C.: Bifurcations and chaos in fractional-order simplified Lorenz system. Int. J. Bifurc. Chaos **20**, 1209–1219 (2010)

46. Diethelm, K.: An algorithm for the numerical solution of differential equations of fractional order. Electron. Trans. Numer. Anal. **5**, 1–6 (1997)

47. Diethelm, K., Ford, N.J.: Analysis of fractional differential equations. J. Math. Anal. Appl. **265**, 229–248 (2002)

48. Diethelm, K., Ford, N.J., Freed, A.D.: A predictor–corrector approach for the numerical solution of fractional differential equations. Nonlinear Dyn. **29**, 3–22 (2002)